Coexistence in Wireless Networks with Heterogeneous Self-interference Cancellation Capabilities

Wessam Afifi[1], Mohammad J. Abdel-Rahman[2], Marwan Krunz[1], and Allen B. MacKenzie[2]

[1]Department of Electrical & Computer Engineering
University of Arizona
{wessamafifi, krunz}@email.arizona.edu

[2]Department of Electrical & Computer Engineering
Wireless @ Virginia Tech
{mo7ammad, mackenab}@vt.edu

***Abstract*—Recently, tremendous progress has been made in self-interference cancellation (SIC) techniques that enable a wireless device to transmit and receive data simultaneously on the same frequency channel, a.k.a. in-band full-duplex (FD) communications. Although operating in a FD mode significantly improves the throughput of a single wireless link, it doubles the number of concurrent transmissions, which limits the potential for coexistence between multiple FD-enabled links. In this paper, we consider the problem of concurrent transmissions between two FD-enabled links with different SIC capabilities; each link can operate in either FD or half-duplex (HD) mode. Following a game-theoretic framework, we aim to determine the stable behavior (FD or HD) for the two coexisting links. To achieve this objective, we first analyze a simple normal form game between the two links, which provides some insight into the coexistence problem. It turns out that the outcome of this game depends on two factors: The amount of residual self-interference (due to imperfect SIC) and the external interference from one link on the other. To capture the impact of residual self-interference, we formulate a Bayesian game between two links with heterogeneous SIC capabilities. In this game, each link (player) tries to maximize its throughput while minimizing the transmission power cost. We derive the Bayesian Nash equilibrium for this game. Furthermore, we determine the conditions on the external interference under which no outage occurs at both links. Finally, we conduct simulations and USRP hardware experiments to corroborate our analytical findings.**

I. Introduction

A. Motivation

Classical wireless systems achieve bidirectional communications by separating the forward and reverse links in time, i.e., time division duplexing (TDD), or frequency, i.e., frequency division duplexing (FDD). Some wireless systems, such as 4G LTE, support both schemes (e.g., LTE-TDD and LTE-FDD). The challenge of achieving simultaneous transmission and reception on the same frequency, i.e., in-band full-duplex (FD) communications, is related to the strong self-interference that arises when a device that is receiving some information signal attempts to transmit another signal at the same time. Because of path loss, the received power of the intended signal (from the peer node) is often much weaker than the node's self-interference. This results in saturating the ADC and prevents packet decoding. Recently, new designs for analog and digital self-interference cancellation (SIC) techniques have been proposed (see [1] for a survey), which together provide up to 110 dB SIC on a single-antenna FD transceiver [2].

From one link's perspective, the advantage of FD communications is clear; it basically doubles the link's throughput. However, such gain is less obvious in the case of a network with multiple interfering links. When these links operate in the same vicinity (i.e., the same collision domain), it is not always optimal for all links to operate in FD fashion [1, 3]. To illustrate, consider the three scenarios in Figure 1. In each scenario, two links are active at the same time and over the same frequency channel. As shown in Figure 1(a), transmitting in an HD fashion enables both links $a \rightarrow b$ and $c \rightarrow d$ to operate simultaneously over the same channel, achieving a total throughput of $2R$ bps (for simplicity, in this example we assume that all transmissions are associated with a constant rate R). However, if link $a \rightarrow b$ switches unilaterally from HD to FD, as shown in Figure 1(b), collisions may occur at both nodes a and d, reducing the network throughput to R bps (only $a \rightarrow b$ transmission is successful). The same argument applies if link $c \rightarrow d$ switches to FD mode instead of $a \rightarrow b$. If both links operate in FD mode, collisions will occur at all four nodes, reducing the network throughput to zero (see Figure 1(c)). Note that this is a simplified example of a small network with only two links. The situation worsens with a higher number of links, where the collision probability increases between concurrent transmissions from different links.

B. Related Work

The feasibility of network-wide FD communications has been discussed in [3–7]. In [3], the authors proposed an analytical framework to analyze the capacity gain of FD networks, assuming a CSMA-based MAC protocol. They found that spatial reuse and inter-link interference may cause significant reduction to the network capacity. To enable FD Wi-Fi networks, the authors in [4] proposed a MAC protocol and presented an experimental and simulation study to assess the performance of their scheme. In contrast to [3], they found that FD communications can potentially enhance the performance of Wi-Fi networks. The authors in [6] considered the inter-node interference in a three-node (base station, downlink node, and uplink node) FD OFDM network. To maximize the network

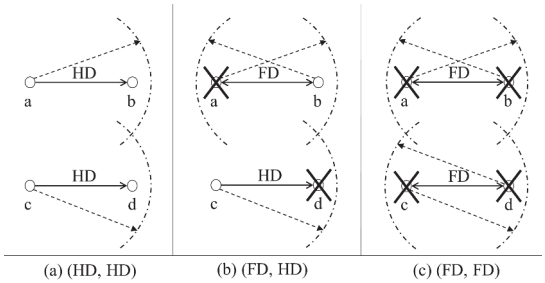

Fig. 1. Implications of operating wireless networks in FD fashion. (a) (HD, HD) strategy returns total throughput of $2R$ bps, (b) (FD, HD) strategy returns total throughput of R bps, while (c) (FD, FD) strategy returns zero throughput. The arcs represent the transmission ranges of different nodes.

sum-throughput under this scenario, they proposed different power allocation schemes while taking into account inter-node interference.

The achievable throughput of FD MIMO networks was investigated in [5, 7]. In [5] the authors considered a binary interference model of a general network topology and derived the conditions under which different technologies (MIMO, multi-user MIMO, and FD communications) achieve the best performance. In [7] the authors considered the problem of power minimization in an FD MIMO network subject to rate demands. They derived conditions under which the FD mode outperforms the HD mode. In [8, 9], the authors investigated the incorporation of SIC techniques in opportunistic spectrum access (OSA) systems, where secondary users (SUs) operate in either simultaneous transmit-receive mode or simultaneous transmit-sense mode, assuming an overlay model. On the other hand, in an underlay OSA network, SUs operate in either HD or FD mode. The authors in [8, 9] determined the optimal operating mode for both overlay and underlay settings.

In [10], the authors proposed several stochastic resource allocation formulations to minimize the cost of composing a virtual LTE-U network from a hybrid set of HD/FD Wi-Fi access points (APs). An AP is assumed to be either HD or FD (with perfect SIC). In general, different devices in a network may have different SIC capabilities, depending, mainly, on the employed analog and digital cancellation mechanisms. In [11] the authors proposed joint channel and base station (BS) stochastic allocation schemes for opportunistic LTE networks with heterogeneous SIC capabilities at different BSs. The resource allocation schemes in [10, 11] are centralized with high computational complexity. Instead, in this paper we develop a game-theoretic framework to analyze the performance of wireless networks with heterogeneous SIC capabilities and in the absence of any global information (i.e., a link does not know the exact SIC level of its neighboring link).

C. Contributions

1) We analyze a simple (HD vs. FD) game between two bidirectional links to gain insight into the coexistence problem. In this game, links (players) know the exact SIC capabilities of each other. Simple utilities and interference models are considered. We find that the outcome of this game depends on two factors: Residual self-interference (RSI) (due to imperfect SIC) and external interference (from one link on the other).
2) To capture the heterogeneity in SIC capabilities, we then formulate a Bayesian game between the two links. In this game, the SIC capability of each link specifies its 'type,' which is unknown to the other link. We derive the Bayesian Nash equilibrium (NE) for this game. From our analysis, we observe that the range of possible SIC values a given player may take can be divided into three regions (types). In two types, either the HD or the FD strategy is dominant, while the Bayesian NE in the third type depends mainly on the probability distribution of the other player's types. Second, the thresholds that specify the regions of various SIC types depend, among other factors, on the outage probabilities of the player's forward and reverse links. Accordingly, we derive closed-form expressions for these thresholds under different outage scenarios.
3) Finally, we conduct simulations and hardware experiments using NI USRP 2922 radios to corroborate our analytical findings.

The rest of the paper is organized as follows. We describe the simple two-player strategic game in Section II. The Bayesian game is formulated and analyzed in Section III. The proposed games are simulated and implemented in Section IV. Finally, in Section V we conclude the paper and provide directions for future research. Due to space limit, some results are omitted, but can be found in an online technical report [12].

II. Simple HD vs. FD Game

In this section, we study a simple strategic game between two coexisting links to identify their stable operational modes. We assume that the two players (links) know all the parameters of the game, including the SIC capability of the other player. Furthermore, we consider simple utility functions and interference models. The game can be defined in the strategic form as $\mathcal{G}_s = (\mathcal{P}, \mathcal{S}, \mathcal{U})$, where:

- $\mathcal{P} = \{P_1, P_2\}$ is the set of players. Let a and b be the two nodes associated with P_1, and let c and d be the two nodes associated with P_2.
- $\mathcal{S} = \{S_1, S_2\}$, where $S_i = \{\text{FD, HD}\}$ is the set of pure strategies of $P_i, i = 1, 2$. An FD strategy of a given player indicates that both nodes of that player will transmit simultaneously on the same channel. On the other hand, under an HD strategy, only a single node (node a in case of P_1 and node c in case of P_2) will transmit data to its peer.
- $\mathcal{U} = \{U_1, U_2\}$, where U_i is the utility of P_i, a map giving the total throughput of link i under each strategy profile.

The utilities of the two links, and hence their operational modes at the NE, depend on two factors: External interference from one link to the other and self-interference. The amount of external interference depends on the channel gains and the transmission powers, whereas self-interference is function of the SIC capabilities. Let R be the throughput of a link in one direction when the communication is successful. Table I shows two instances of the game $\mathcal{G}_s$. In the first instance (Table I(a)), both external and self-interference are assumed to be high. As a result, if both P_1 and P_2 operate in the FD mode, then their utilities will be zero. Although (FD, FD) is a NE, it is not an efficient one. Moreover, (FD, FD) is not a unique NE. Specifically, (FD, HD) and (HD, FD) are also NE and, in fact, they are Pareto efficient. In another instance of $\mathcal{G}_s$ (shown in

TABLE I. UTILITIES IN THE SIMPLE GAME.

(a) High external and self-interference

P_1 \ P_2	FD	HD
FD	$(0, 0)$	$(2R, 0)$
HD	$(0, 2R)$	(R, R)

(b) Low external interference and perfect SIC

P_1 \ P_2	FD	HD
FD	(2R, 2R)	(2R, R)
HD	(R, 2R)	(R, R)

Table I(b)), the external interference is low and all nodes have perfect SIC. In this case, (FD, FD) is an efficient and unique NE.

The above game illustrates that FD communications is not always optimal from a network's perspective. To provide a complete characterization of the stable strategy profiles for coexisting FD-enabled links, we account for nodes' SIC capabilities as well as the amount of induced interference from one link on the other in the following Bayesian game.

III. GAME WITH HETEROGENEOUS SIC CAPABILITIES

A. Game Formulation

The two-player Bayesian game can be defined as $\mathcal{G} = (\mathcal{P}, \mathcal{S}, \Theta, \mathcal{U}, \mathcal{D})$, where $\mathcal{P}$ and $\mathcal{S}$ are as in $\mathcal{G}_s$. The exact expressions for the utility set $\mathcal{U} = \{U_1, U_2\}$ will be defined later. As for Θ and $\mathcal{D}$, they are defined as follows:

- $\Theta = \{\Theta_1, \Theta_2\}$, where $\Theta_i = \{1, 2, 3\}$ is the set of types of P_i. Here, the type represents a range of values for the SIC capability of P_i that dictates a certain strategy. Let $\chi_i \in [0, 1]$ be the SIC parameter of P_i. For simplicity, we assume that both nodes of P_i have the same χ_i. Specifically, χ_i is the ratio between the RSI signal and the original one. If $\chi_i = 0$, the corresponding node can totally suppress its self-interference signal (perfect SIC); otherwise, it can only suppress a fraction $1-\chi_i$ of its self-interference. As we later show, the outcome of the game does not depend on the exact value of χ_i, but rather the relationships between χ_i and two thresholds, χ_i^* and χ_i^{**}, to be derived. As a result, P_i will be of one of three types: Type 1 ($\theta_i = 1$), type 2 ($\theta_i = 2$), and type 3 ($\theta_i = 3$).
- $\mathcal{D} = \{D_1, D_2\}$, where D_i is a probability distribution over the types of $P_i, i = 1, 2$. P_i is of type 1 with probability p_{i1}, of type 2 with probability p_{i2}, and of type 3 with probability p_{i3}. Note that θ_1 and θ_2 are independent.

Finally, in Bayesian games a pure strategy of P_i is a map s_i: $\Theta_i \rightarrow S_i$, prescribing an action for each type of P_i. Strategy spaces, player types, utility functions, and the probability distributions over the types are assumed to be common knowledge to all players. However, a given player knows only its current strategy and type, and does not know the strategies selected by the other player or its true type.

Next, we analyze the utility U_1 for P_1 (U_2 can be analyzed similarly). First, consider U_1 under the (FD, FD) strategy profile. P_1 benefits from an FD transmission only if no outage/collision occurs at the receivers of a and b, i.e., when $\gamma_{ij}^{(\text{FF})} \geq \gamma_{ij}^*, i, j \in \{a, b\}$, where $\gamma_{ij}^{(\text{FF})}$ is the SNR at node j while receiving data from node i under (FD, FD) and γ_{ij}^* is a given reception threshold. Define $\mathbb{1}_{ij}^{(\text{FF})}$ to be an indicator function for a transmission from i to j under (FD, FD). $\mathbb{1}_{ij}^{(\text{FF})} = 1$ if $\gamma_{ij}^{(\text{FF})} \geq \gamma_{ij}^*$ and 0 otherwise. Denote the transmission cost from i to j by C_{ij}. We set $C_{ij} = c_{ij} P_{t,i}$, where $P_{t,i}$ is the transmission power of node $i, i \in \{a, b, c, d\}, j \in \{a, b\}$, and c_{ij} is a constant. Then, the utility of P_1 under (FD, FD), denoted by $U_1^{(\text{FF})}$, can be expressed as follows:

$$U_1^{(\text{FF})} = \mathbb{1}_{ab}^{(\text{FF})} R_{ab}^{(\text{FF})} + \mathbb{1}_{ba}^{(\text{FF})} R_{ba}^{(\text{FF})} - C_{ab} - C_{ba} \tag{1}$$

where $R_{ab}^{(\text{FF})}$ and $R_{ba}^{(\text{FF})}$ are, respectively, the forward and reverse link throughputs for link (a, b). $R_{ij}^{(\text{FF})}$, $i, j \in \{a, b\}, i \neq j$, is given by:

$$\begin{aligned} R_{ij}^{(\text{FF})} &= \log\left(1 + \gamma_{ij}^{(\text{FF})}\right) \\ &= \log\left(1 + \frac{P_{t,i} g_{ij}}{\chi_j^2 P_{t,j} g_{jj} + P_{t,c} g_{cj} + P_{t,d} g_{dj} + \sigma_j^2}\right) \end{aligned} \tag{2}$$

where g_{ij} is the channel gain between any two nodes i and $j, i \neq j$, and σ_j^2 is the noise power at node j. The notation g_{jj} indicates the self-interference channel gain at node j. Note the RSI term in the denominator of the SNR. According to our earlier assumption, $\chi_a = \chi_b \triangleq \chi_1$ (also, $\chi_c = \chi_d \triangleq \chi_2$).

Under (HD, FD) (i.e., P_1 selects HD while P_2 selects FD), P_1's utility, denoted by $U_1^{(\text{HF})}$, includes the throughput of the forward link only minus its transmission cost. The same amount of external interference is still induced on P_1, as P_2 still operates in FD mode. Formally, $U_1^{(\text{HF})}$ can be written as:

$$U_1^{(\text{HF})} = \mathbb{1}_{ab}^{(\text{HF})} R_{ab}^{(\text{HF})} - C_{ab} = \mathbb{1}_{ab}^{(\text{HF})} \log\left(1 + \gamma_{ab}^{(\text{HF})}\right) - c_{ab} P_{t,a} \tag{3}$$

where $\gamma_{ab}^{(\text{HF})} = P_{t,a} g_{ab} / \left(P_{t,c} g_{cb} + P_{t,d} g_{db} + \sigma_b^2\right)$ is the SNR at b when receiving data from a under (HD, FD).

For the two other strategy profiles, P_1's utility can be written as follows:

$$\begin{aligned} U_1^{(\text{FH})} &= \mathbb{1}_{ab}^{(\text{FH})} \log\left(1 + \gamma_{ab}^{(\text{FH})}\right) - c_{ab} P_{t,a} \\ &+ \mathbb{1}_{ba}^{(\text{FH})} \log\left(1 + \gamma_{ba}^{(\text{FH})}\right) - c_{ba} P_{t,b} \end{aligned} \tag{4}$$

$$U_1^{(\text{HH})} = \mathbb{1}_{ab}^{(\text{HH})} \log\left(1 + \gamma_{ab}^{(\text{HH})}\right) - c_{ab} P_{t,a} \tag{5}$$

where $\gamma_{ab}^{(\text{FH})} = P_{t,a} g_{ab} / \left(\chi_b^2 P_{t,b} g_{bb} + P_{t,c} g_{cb} + \sigma_b^2\right)$, $\gamma_{ba}^{(\text{FH})} = P_{t,b} g_{ba} / \left(\chi_a^2 P_{t,a} g_{aa} + P_{t,c} g_{ca} + \sigma_a^2\right)$, and $\gamma_{ab}^{(\text{HH})} = P_{t,a} g_{ab} / \left(P_{t,c} g_{cb} + \sigma_b^2\right)$.

To find the Bayesian NE, we first define technical conditions under which no outage/collision occurs at the receivers of both players. We start by analyzing the no-outage case to facilitate understanding the Bayesian game analysis. Then, we conclude this section by stating the Bayesian NE in the general case when outage may occur.

Outage will not occur for P_1 iff $\gamma_{ab}^{mn} \geq \gamma_{ab}^*$ and $\gamma_{ba}^{mn} \geq \gamma_{ba}^*, \forall m, n \in S_1$. However, by examining the SNR expressions for different strategy profiles, we notice that the minimum SNR is encountered under (FD, FD) due to the existence of two interference terms from nodes c and d, in addition to the RSI. With the imposed conditions on $\gamma_{ab}^{(\text{FF})}$ and $\gamma_{ba}^{(\text{FF})}$, we implicitly ensure that no outage occurs under the other strategy profiles.

Formally, we define the following two conditions on P_1:

$$\text{TC}_{11}:\ P_{t,c}g_{cb}+P_{t,d}g_{db}-\frac{P_{t,a}g_{ab}}{\gamma^*_{ab}}+\chi_1^2P_{t,b}g_{bb}+\sigma_b^2<0 \quad (6)$$

$$\text{TC}_{12}:\ P_{t,c}g_{ca}+P_{t,d}g_{da}-\frac{P_{t,b}g_{ba}}{\gamma^*_{ba}}+\chi_1^2P_{t,a}g_{aa}+\sigma_a^2<0. \quad (7)$$

Two similar technical conditions can be established for P_2. We later discuss the case when those technical conditions are not satisfied (i.e., an outage may occur). Now, we formally define the three types of player P_i.

- Type 1 ($\chi_i \in [0, \chi_i^*]$): When χ_i is sufficiently small, P_i can efficiently suppress its self-interference signal, ensuring that the FD strategy dominates the HD strategy. χ_1^* is the value of χ_1 at which $U_1^{(\text{FH})} = U_1^{(\text{HH})}$ and χ_2^* is the value of χ_2 at which $U_2^{(\text{HF})} = U_2^{(\text{HH})}$.
- Type 2 ($\chi_i \in (\chi_i^*, \chi_i^{**})$): As χ_i increases, the higher RSI makes the HD strategy more preferable in some cases (especially if the other player is following the HD strategy). This means that P_1's utility, for example, under (FD, HD) decreases faster with χ_1 than that under (FD, FD). The reason for this is that under (FD, HD), the RSI dominates the external interference (since P_2 is playing HD), which is not the case for the (FD, FD). The same argument applies to player P_2. χ_1^{**} is defined as the value of χ_1 at which $U_1^{(\text{FF})} = U_1^{(\text{HF})}$ and χ_2^{**} is defined as the value of χ_2 at which $U_2^{(\text{FF})} = U_2^{(\text{FH})}$.
- Type 3 ($\chi_i \in [\chi_i^{**}, 1]$): As χ_i continues to increase beyond χ_i^{**}, the RSI signal will be very high, forcing the utilities under the FD strategy to be lower than that of the HD strategy (irrespective of the other player's strategy). Towards the end of this section, we discuss how χ_i^* and χ_i^{**} can be computed.

B. Existence and Uniqueness of a Bayesian NE

Theorem 1: Game $\mathcal{G}$ described above has a Bayesian NE (s_1^*, s_2^*), which is given by:

$$s_i^* = \begin{cases} \text{FD}, & \text{if } \theta_i = 1 \\ \begin{cases} \text{FD}, & \text{if } p_{\hat{i}1} > \alpha_i \\ \text{FD (HD)}, & \text{if } p_{\hat{i}1} \le \alpha_i \text{ and } p_{\hat{i}1}+p_{\hat{i}2} \ge \alpha_i \\ \text{HD}, & \text{if } p_{\hat{i}1}+p_{\hat{i}2} < \alpha_i \end{cases}, & \text{if } \theta_i = 2 \\ \text{HD}, & \text{if } \theta_i = 3 \end{cases} \quad (8)$$

for $i \in \{1,2\}$. $\hat{i} = (i \mod 2)+1$ is the index of node i's peer node (i.e., if $i = 1, \hat{i} = 2$, and vice verse). $\alpha_1, \alpha_2 \in [0,1]$ are defined as:

$$\alpha_1 \stackrel{\text{def}}{=} \frac{U_1^{(\text{HH})} - U_1^{(\text{FH})}}{U_1^{(\text{HH})} - U_1^{(\text{FH})} + U_1^{(\text{FF})} - U_1^{(\text{HF})}} \quad (9)$$

$$\alpha_2 \stackrel{\text{def}}{=} \frac{U_2^{(\text{HH})} - U_2^{(\text{HF})}}{U_2^{(\text{HH})} - U_2^{(\text{HF})} + U_2^{(\text{FF})} - U_2^{(\text{FH})}}. \quad (10)$$

Note that α_i is a function of $\chi_i, i \in \{1,2\}$

Proof: If player P_1 is of type 1, then $U_1^{(\text{FF})} > U_1^{(\text{HF})}$ and $U_1^{(\text{FH})} > U_1^{(\text{HH})}$, i.e., the FD strategy strictly dominates the HD strategy. On the other hand, if P_1 is of type 3, then $U_1^{(\text{FF})} < U_1^{(\text{HF})}$ and $U_1^{(\text{FH})} < U_1^{(\text{HH})}$, i.e., the HD strategy strictly dominates the FD strategy. Applying the same argument to player P_2, we can determine the Bayesian NE if the players are of type 1 or 3, as shown in (8).

The more challenging case occurs when at least one of the players is of type 2. If P_1 is of type 2, then $U_1^{(\text{FF})} > U_1^{(\text{HF})}$ and $U_1^{(\text{FH})} < U_1^{(\text{HH})}$. Therefore, P_1's decision depends on P_2's action. As mentioned earlier, P_2's action will be FD if $\theta_2 = 1$ and HD if $\theta_2 = 3$, however, its action when $\theta_2 = 2$ is not determined yet. First, consider the case when P_2's action is FD and $\theta_2 = 2$. In this case, P_1's FD strategy dominates the HD strategy iff:

$$p_{21}U_1^{(\text{FF})}+p_{22}U_1^{(\text{FF})}+p_{23}U_1^{(\text{FH})} > p_{21}U_1^{(\text{HF})}+p_{22}U_1^{(\text{HF})}+p_{23}U_1^{(\text{HH})}.$$

Second, if P_2's action is HD when $\theta_2 = 2$, then P_1's FD strategy dominates the HD strategy iff:

$$p_{21}U_1^{(\text{FF})}+p_{22}U_1^{(\text{FH})}+p_{23}U_1^{(\text{FH})} > p_{21}U_1^{(\text{HF})}+p_{22}U_1^{(\text{HH})}+p_{23}U_1^{(\text{HH})}.$$

Solving the above two equations along with $p_{21}+p_{22}+p_{23}=1$, we obtain the value of α_1 and derive the conditions on P_2's probability distribution as in (8). A similar approach is used to determine α_2 for P_2. ■

Corollary 1: If each of the two players P_1 and P_2 satisfies one of the following two conditions:

$$p_{\hat{i}1} > \alpha_i \quad (11)$$

$$p_{\hat{i}1}+p_{\hat{i}2} < \alpha_i \quad (12)$$

where $i \in \{1,2\}$ and $\hat{i} = (i \mod 2)+1$, then, game $\mathcal{G}$ has a unique Bayesian NE. That is given by:

$$((\text{F},\text{F},\text{H}),(\text{F},\text{F},\text{H})) \quad \text{if} \quad p_{21} > \alpha_1 \ \&\ p_{11} > \alpha_2 \quad (13)$$

$$((\text{F},\text{F},\text{H}),(\text{F},\text{H},\text{H})) \quad \text{if} \quad p_{21} > \alpha_1 \ \&\ p_{11}+p_{12} < \alpha_2 \quad (14)$$

$$((\text{F},\text{H},\text{H}),(\text{F},\text{F},\text{H})) \quad \text{if} \quad p_{21}+p_{22} < \alpha_1 \ \&\ p_{11} > \alpha_2 \quad (15)$$

$$((\text{F},\text{H},\text{H}),(\text{F},\text{H},\text{H})) \quad \text{if} \quad p_{21}+p_{22} < \alpha_1 \ \&\ p_{11}+p_{12} < \alpha_2 \quad (16)$$

where the notation $((\text{F},\text{F},\text{H}),(\text{F},\text{H},\text{H}))$, for instance, means that P_1 operates in the FD mode when $\theta_1 = 1$ or 2 and in the HD mode when $\theta_1 = 3$, while P_2 operates in the FD mode when $\theta_2 = 1$ and in the HD mode when $\theta_2 = 2$ or 3.

Proof: The two-player Bayesian game $\mathcal{G}$ (with each player having one of three possible types) can be equivalently formulated as a 2^3 by 2^3 strategic game. From Theorem 1 and its proof, it can be shown that under each of the conditions stated in (13)-(16), the corresponding strategy profile consists of a strictly dominating strategy for each player in the 8-by-8 game. Hence, the Bayesian NE is unique. ■

Corollary 2: If exactly one of the players neither satisfies (11) nor (12), then the game $\mathcal{G}$ has two Bayesian NEs (from the strategy profiles given by (13)-(16)).

Proof: Follows from Theorem 1 and Corollary 1. ■

Corollary 3: If both players neither satisfy (11) nor (12), then the game has the four Bayesian NEs, given by (13)-(16).

Proof: Follows from Theorem 1 and Corollary 1. ■

C. Accounting for Link Outages

We now relax the technical conditions ((6) and (7) for P_1 and the two similar conditions for P_2), and assume that any of the forward/reverse links may experience outage. In this case, the relation between χ_i^* and χ_i^{**} is not fixed (i.e., χ_i^* could be larger or smaller than χ_i^{**}). The reason is that in the case of outage, if P_2 operates in the FD mode, then $U_1^{(\text{FF})}$ may decrease faster with χ_1 compared to $U_1^{(\text{FH})}$, and hence the condition $U_1^{(\text{FF})} = U_1^{(\text{HF})}$ may be satisfied before the condition $U_1^{(\text{FH})} = U_1^{(\text{HH})}$. Therefore, $\chi_1^{**} < \chi_1^*$ (recall the definition of χ_1^* and χ_1^{**} in Section III-A). The same situation arises in the case of P_2 when outage is likely to happen.

Theorem 2: Theorem 1 and Corollaries 1-3 hold true for game $\mathcal{G}$ under the possibility of outage. However, $\theta_i, i \in \{1,2\}$, in this case, is given by:

$$\theta_i = \begin{cases} 1, & \text{if } \chi_i \leq \min(\chi_i^*, \chi_i^{**}) \\ 2, & \text{if } \min(\chi_i^*, \chi_i^{**}) < \chi_i < \max(\chi_i^*, \chi_i^{**}) \\ 3, & \text{if } \chi_i \geq \max(\chi_i^*, \chi_i^{**}). \end{cases} \tag{17}$$

Proof: From the definitions of χ_i^* and χ_i^{**} in Section III-A, it can be shown that, irrespective whether outage occurs or not, the dominating strategy of player P_i when $\chi_i \leq \min(\chi_i^*, \chi_i^{**})$ is FD, and when $\chi_i \geq \max(\chi_i^*, \chi_i^{**})$ is HD. When $\min(\chi_i^*, \chi_i^{**}) < \chi_i < \max(\chi_i^*, \chi_i^{**})$, following the same approach in the proof of Theorem 1 (by deriving the conditions under which P_i's expected utility under the FD strategy is higher than that under the HD strategy while fixing the other player strategy, and solving the two resulting inequalities along with $p_{21} + p_{22} + p_{23} = 1$, it can be shown that the dominating strategy is given by (8) when $\theta_i = 2$. Hence, Theorem 2 holds. ■

Next, we provide closed-form expressions for χ_1^* and χ_1^{**} (the derivations of these expressions along with similar expressions for χ_2^* and χ_2^{**} can be found in an online technical report [12]):

$$\chi_1^* = \begin{cases} 0, & \text{if } \mathbb{1}_{ab}^{(\text{FH})} = \mathbb{1}_{ba}^{(\text{FH})} = 0 \\ \sqrt{\left(\frac{1}{P_{t,a} g_{aa}}\right)\left(\frac{P_{t,b} g_{ba}}{e^w - 1} - v\right)}, & \text{if } \mathbb{1}_{ab}^{(\text{FH})} = 0,\ \mathbb{1}_{ba}^{(\text{FH})} = 1 \\ \sqrt{\left(\frac{1}{P_{t,b} g_{bb}}\right)\left(\frac{P_{t,a} g_{ab}}{e^w - 1} - u\right)}, & \text{if } \mathbb{1}_{ab}^{(\text{FH})} = 1,\ \mathbb{1}_{ba}^{(\text{FH})} = 0 \\ \sqrt{\frac{-\beta_2 - \sqrt{\beta_2^2 - 4\beta_1\beta_3}}{2\beta_1}}, & \text{if } \mathbb{1}_{ab}^{(\text{FH})} = \mathbb{1}_{ba}^{(\text{FH})} = 1 \end{cases}$$

where $w \overset{\text{def}}{=} \mathbb{1}_{ab}^{(\text{HH})} R_{ab}^{(\text{HH})} + C_{ba}$, $u \overset{\text{def}}{=} P_{t,c} g_{cb} + \sigma_b^2$, $v \overset{\text{def}}{=} P_{t,c} g_{ca} + \sigma_a^2$, $\beta_1 = P_{t,a} P_{t,b} g_{aa} g_{bb} (1 - e^w)$, $\beta_2 = (P_{t,b} g_{bb} v + P_{t,a} g_{aa} u)(1 - e^w) + P_{t,b}^2 g_{ba} g_{bb} + P_{t,a}^2 g_{ab} g_{aa}$, and $\beta_3 = uv(1 - e^w) + P_{t,b} g_{ba} u + P_{t,a} g_{ab} v + P_{t,a} P_{t,b} g_{ab} g_{ba}$.

$$\chi_1^{**} = \begin{cases} 0, & \text{if } \mathbb{1}_{ab}^{(\text{FF})} = \mathbb{1}_{ba}^{(\text{FF})} = 0 \\ \sqrt{\left(\frac{1}{P_{t,a} g_{aa}}\right)\left(\frac{P_{t,b} g_{ba}}{e^{\hat{w}} - 1} - \hat{v}\right)}, & \text{if } \mathbb{1}_{ab}^{(\text{FF})} = 0,\ \mathbb{1}_{ba}^{(\text{FF})} = 1 \\ \sqrt{\left(\frac{1}{P_{t,b} g_{bb}}\right)\left(\frac{P_{t,a} g_{ab}}{e^{\hat{w}} - 1} - \hat{u}\right)}, & \text{if } \mathbb{1}_{ab}^{(\text{FF})} = 1,\ \mathbb{1}_{ba}^{(\text{FF})} = 0 \\ \sqrt{\frac{-\hat{\beta}_2 - \sqrt{\hat{\beta}_2^2 - 4\hat{\beta}_1\hat{\beta}_3}}{2\hat{\beta}_1}}, & \text{if } \mathbb{1}_{ab}^{(\text{FF})} = \mathbb{1}_{ba}^{(\text{FF})} = 1 \end{cases}$$

where $\hat{u} \overset{\text{def}}{=} P_{t,c} g_{cb} + P_{t,d} g_{db} + \sigma_b^2$, $\hat{v} \overset{\text{def}}{=} P_{t,c} g_{ca} + P_{t,d} g_{da} + \sigma_a^2$, $\hat{w} \overset{\text{def}}{=} \mathbb{1}_{ab}^{(\text{HF})} R_{ab}^{(\text{HF})} + C_{ba}$, $\hat{\beta}_1 = P_{t,a} P_{t,b} g_{aa} g_{bb} (1 - e^{\hat{w}})$, $\hat{\beta}_2 = (P_{t,b} g_{bb} \hat{v} + P_{t,a} g_{aa} \hat{u})(1 - e^{\hat{w}}) + P_{t,b}^2 g_{ba} g_{bb} + P_{t,a}^2 g_{ab} g_{aa}$, and $\hat{\beta}_3 = \hat{u}\hat{v}(1 - e^{\hat{w}}) + P_{t,b} g_{ba} \hat{u} + P_{t,a} g_{ab} \hat{v} + P_{t,a} P_{t,b} g_{ab} g_{ba}$.

IV. Performance Evaluation

In this section, we conduct numerical evaluations, LabVIEW simulations, and hardware experiments to assess the performance of our proposed game-theoretic analysis.

A. Numerical Results

For the numerical results, unless stated otherwise, we use the following parameter values: The channel gain between nodes i and j, g_{ij}, is set to $1, \forall i, j \in \{a, b, c, d\}$, $\sigma_i^2 = 1$ Watt, and the normalized transmission cost c_{ij} is set 0.001.

Figure 2 depicts the expected utility for P_1 vs. χ_1 at different values of *interference channel gains* (ICGs) (i.e., channel gains between the transmitters of P_1 and receivers of P_2, and vice versa). As shown in the figure, increasing the ICGs reduces the expected utility of P_1. If P_1 is of type 1, its expected utility decreases with χ_1, as P_1 operates in the FD mode, whereas when it is of type 3, its expected utility is constant because it operates in the HD mode. When P_1 is of type 2, P_1 starts operating in the FD mode as χ_1 increases (since $p_{21} > \alpha_1$), and eventually it switches to the HD mode when α_1 exceeds p_{21}. As shown in the figure, the expected utility when $\theta_1 = 2$ first decreases with χ_1 and then switches to a fixed value. Note that the SIC thresholds are different for different ICGs (we only show these thresholds when ICG$= 0.01$). In Figure 3, we show P_1's expected utility for different values of p_{21} (apriori probability that P_2 is of type 1). As p_{21} increases, P_1's expected utility decreases. The reason is that if p_{21} is sufficiently small (e.g., $p_{21} = 0.1$), the expected interference level is relatively low and hence higher expected utility can be achieved.

Figure 4 shows the SIC thresholds of players P_1 and P_2 vs. $P_{t,c}$. Under conditions (6) and (7) for P_1 and the two similar conditions for P_2, $\chi_i^* < \chi_i^{**}, \forall i$. Since $P_{t,c}$ is the dominating term in $\gamma_{ab}^{(\text{HH})}$, increasing $P_{t,c}$ causes $U_1^{(\text{HH})}$ to decrease faster than $U_1^{(\text{FH})}$. Hence, χ_1^* increases with $P_{t,c}$. A similar argument can be made regarding χ_1^{**}. On the other hand, increasing $P_{t,c}$ causes $U_2^{(\text{HF})}$ to decrease faster than $U_2^{(\text{HH})}$. Hence, χ_2^* decreases with $P_{t,c}$. In the technical report [12], we plot the players' expected utilities vs. p_{21} for different values of p_{11}.

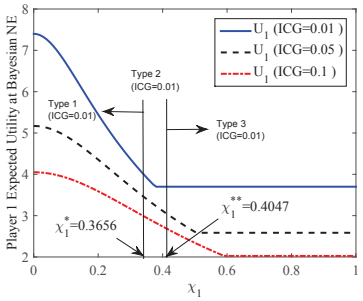

Fig. 2. P_1's expected utility at Bayesian NE vs. χ_1 ($\chi_2 = 0$, uniform distribution over the types of both players, and $P_{t,i} = 100$ Watts $\forall i$).

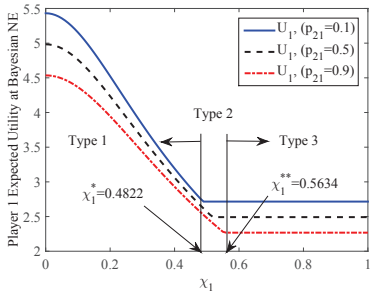

Fig. 3. P_1's expected utility at Bayesian NE vs. χ_1 ($\chi_2 = 0$, uniform distribution over P_1 types, $p_{22} = p_{23} = (1 - p_{21})/2$, ICGs= 0.05, and $P_{t,i} = 100$ Watts $\forall i$).

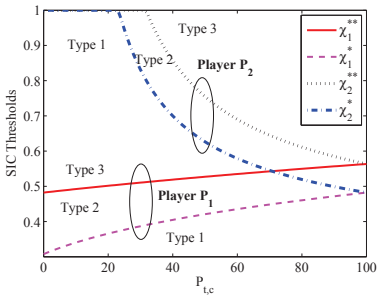

Fig. 4. SIC thresholds for P_1 and P_2 vs. $P_{t,c}$ (ICGs= 0.05 and $P_{t,i} = 100$ Watts $\forall i$).

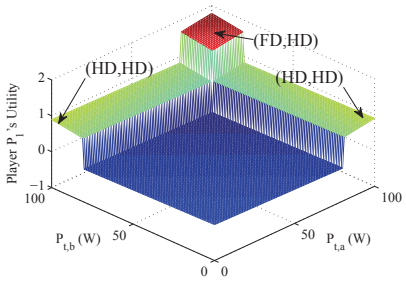

Fig. 5. Player P_1's throughput vs. its transmission powers, $P_{t,a}$ and $P_{t,b}$ ($\chi_1 = 0$, P_2 operates in the HD mode, and $P_{t,c} = 100$ Watts).

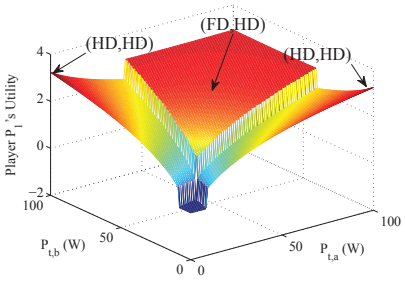

Fig. 6. Player P_1's throughput vs. its transmission powers, $P_{t,a}$ and $P_{t,b}$ ($\chi_1 = 0.4$, P_2 operates in the HD mode, and $P_{t,c} = 100$ Watts).

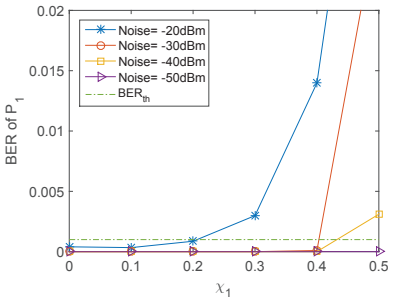

Fig. 7. Forward-link BER of P_1 vs. χ_1 at different noise levels (no external interference, simulations).

In the next two figures, we consider the case where an outage may occur at the receiver of any player. Even with complete SIC, when both players operate in the FD mode, outage may occur at all receivers, resulting in negative utilities for both players (because of the transmission costs). However, when P_2 operates in the HD mode, P_1 starts getting a positive utility, as shown in Figure 5. Note that P_1 doubles its throughput in the (FD, HD) strategy profile compared to (HD, HD) when the maximum transmission power is used. However, as P_1's transmission power decreases, outage occurs. Figure 6 shows the case when $\chi_1 = 0.4$. In this case, P_1's utility under (HD, HD) with $P_{t,c} = 10$ Watts is higher than that under (FD, HD). This is due to the increase in the level of RSI.

B. LabVIEW Simulations

For simulations, LabVIEW 2014 software, developed by National Instruments, is used to acquire, analyze, and visualize data. The simulation setup is as follows. We consider a single-channel FD network consisting of two links with different SIC capabilities. Each link can operate in the HD or FD modes. For transmission, we generate back-to-back packets, each consisting of 500 bits, modulated using QPSK and a code rate of $1/2$. We then add control information (e.g., training sequence) and pass them to the pulse shaping block for transmission. The simulation parameters are the mean of the Gaussian noise (varies from -20 dBm to -50 dBm), the ICGs $= \{0.01, 0.04, 0.09\}$, and SIC capabilities (0 to 0.5). We focus on the more practical case, where χ_i value is low. Both, the players' channel coefficient and the self-interference channel coefficient is fixed at $0.707 + 0.707i$ (gain $= 1$). For each simulation run, we take the average of 1000 iterations (i.e., 1000 back-to-back packets). We fix the channel phase to $\pi/4$ and set the BER threshold needed for correct reception to $\text{BER}_{\text{th}} = 10^{-4}$.

Figure 7 shows the forward-link BER of P_1 vs. χ_1 at different noise levels when P_2 is not operating (switched off). Depending on the noise level and the SIC capability, P_1 decides to operate in the HD or FD modes. This figure shows the effect of RSI (due to incomplete SIC) on the BER of P_1. As expected, the BER of P_1 increases with χ_1. Specifically, P_1 operates in the FD mode for all values of χ_1 at which the average BER is lower than BER_{th}. Once the average BER exceeds BER_{th} (i.e., the receiver is not able to decode the packet), the optimal communication mode for P_1 becomes HD. As shown in Figure 7, the threshold value of χ_1 for switching from FD to HD decreases with the noise level; when the noise equals -50 dBm, this threshold equals 1 (i.e., P_1 always operates in the FD mode), whereas when the noise equals -20 dBm, this threshold equals 0.2 (i.e., P_1 operates in the FD mode if $\chi_1 < 0.2$ and operates in the HD mode otherwise).

Figures 8 and 9 show the forward-link BER of P_1 vs. χ_1 at different noise levels, when P_2 operates in the FD and HD modes, respectively. In these two figures, channel coefficients are $0.0707 + 0.0707i$ (ICGs $= 0.01$). As expected, the threshold values of χ_1 under the (FD, FD) strategy profile are lower than those under (FD, HD) for the same noise levels. This means that the range of SIC capabilities for P_1 to operate in the FD mode is narrower when P_2 operates in the FD mode compared to the case when P_2 operates in the HD mode. The

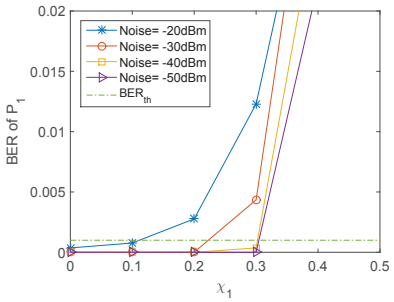

Fig. 8. Forward-link BER of P_1 vs. χ_1 at different noise levels. P_2 operates in the FD mode (ICGs $= 0.01$, simulations).

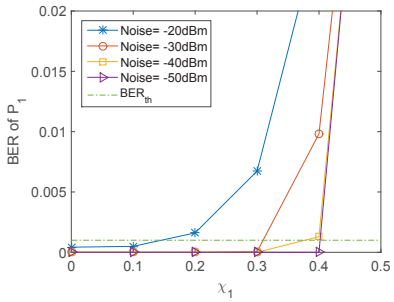

Fig. 9. Forward-link BER of P_1 vs. χ_1 at different noise levels. P_2 operates in the HD mode (ICG $= 0.01$, simulations).

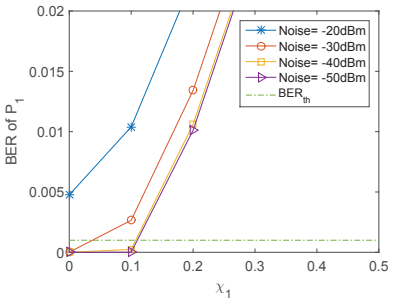

Fig. 10. Forward-link BER of P_1 vs. χ_1 at different noise levels. P_2 operates in the FD mode (ICGs $= 0.04$, simulations).

reason for this is that when P_2 operates in the FD mode, it induces higher interference on P_1 than when it operates in the HD mode, which causes outage to occur sooner at P_1 (i.e., at smaller values of χ_1). Comparing Figure 7 to Figures 8 and 9, the range of χ_1 under which P_1 operates in the FD mode is higher when link P_2 is switched off compared to the case when it is on. We repeat the above setup for different ICG values (see the online technical report [12] for more simulation results). We present a sample result in Figure 10, which shows the forward-link BER of P_1 vs. χ_1 at different noise levels, when P_2 operates in the FD mode. In this figure, channel coefficients are $0.1414 + 0.1414i$ (ICG $= 0.04$). Similar conclusions can be made regarding the regions of the FD and HD modes for P_1 as the ICGs increase.

Figure 11 shows the received signal constellation at P_1 for different noise levels and SIC capabilities, when P_2 is switched off. Specifically, Figures 11(a), 11(b), and 11(c) show the received constellation when the noise level is -50 dBm and $\chi_1 = 0, 0.1$, and 0.2, respectively. As χ_1 increases, the variance of the received constellation points increase due to the RSI signal, and as a result the BER increases. Figures 11(d), 11(e), and 11(f) show similar constellation graphs, but at a higher noise level ($= -20$ dBm). Figure 12 shows another set of sub-figures for the received constellation when P_2 operates in the FD mode. Both channel coefficients are $0.0707 + 0.0707i$. The external interference from the bi-directional link of P_2 increases the variance of the received constellation points. These interferences, along with the RSI, cause the BER of P_1 to increase. As a result, in some cases (depending on the noise level), P_1 will switch to the HD mode.

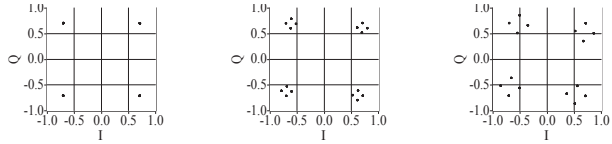

(a) Noise $= -50$ dBm and $\chi_1 = 0$ (b) Noise $= -50$ dBm and $\chi_1 = 0.1$ (c) Noise $= -50$ dBm and $\chi_1 = 0.2$

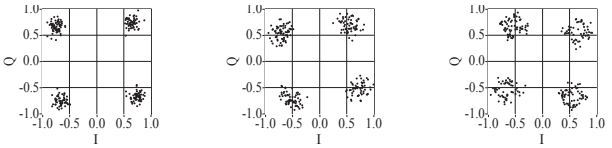

(d) Noise $= -20$ dBm and $\chi_1 = 0$ (e) Noise $= -20$ dBm and $\chi_1 = 0.1$ (f) Noise $= -20$ dBm and $\chi_1 = 0.2$

Fig. 11. Received signal constellation at different noise levels and SIC capabilities (no external interference, simulations).

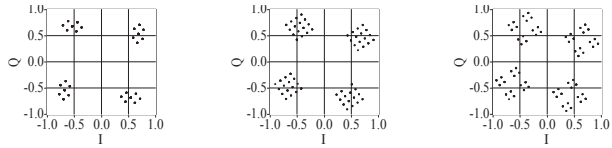

(a) Noise $= -50$ dBm and $\chi_1 = 0$ (b) Noise $= -50$ dBm and $\chi_1 = 0.1$ (c) Noise $= -50$ dBm and $\chi_1 = 0.2$

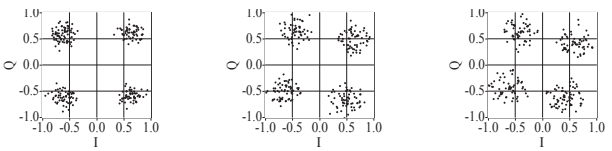

(d) Noise $= -20$ dBm and $\chi_1 = 0$ (e) Noise $= -20$ dBm and $\chi_1 = 0.1$ (f) Noise $= -20$ dBm and $\chi_1 = 0.2$

Fig. 12. Received signal constellation at different noise levels and SIC capabilities. P_2 operates in the FD mode (ICGs $= 0.01$, simulations).

C. Hardware Experiments

The experimental setup is shown in Figure 13. We consider two coexisting links represented by four NI USRP 2922 radios. These USRPs are connected via Ethernet cables to two host PCs, running LabVIEW 2014. For transmission, we generate back-to-back packets, with packet length of 500 bits, which are modulated as 250 symbols using QPSK. We then add control information (e.g., training sequence) and pass them to the pulse shaping block. These complex I and Q symbols are then transmitted to the USRP device via the Ethernet cable. At the USRP device, the transmitter chain starts with the digital up-conversion (DUC) block, which passes the signal to the DAC. After that, an I-Q mixing occurs to directly up-convert the signal and produce an RF signal that is amplified and transmitted over the 2.4 GHz band (transmission power is around 0 dbm).

To enable FD communications, each node/USRP is equipped with two antennas, one for transmission and the other for reception. We use antenna separation [13] to separate the transmit and receive signals in the space domain. To further reduce the level of self-interference, we also exploit the antenna gain pattern by using directional antennas. In total, we achieve around 70 dB reduction in self-interference.

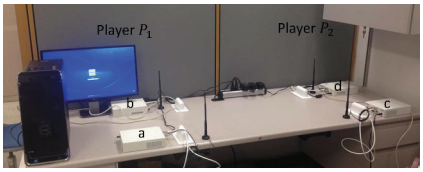

Fig. 13. Experimental setup. P_1 consists of nodes a and b. P_2 consists of nodes c and d.

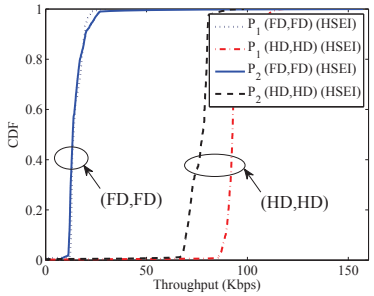

Fig. 14. Throughput CDF under the (FD, FD) and (HD, HD) strategies in the HSEI case.

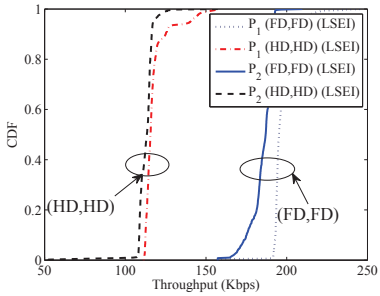

Fig. 15. Throughput CDF under the (FD, FD) and (HD, HD) strategies in the LSEI case.

We conduct two types of experiments. First, we test the *high self- and external interference* (HSEI) case, where we place the four USRPs close to each other inside the lab. Furthermore, we displace the antennas from their optimal position so that the amount of RSI is relatively high. We then operate our network in two modes: (FD, FD) and (HD, HD), for a duration of 500 back-to-back packets. Figure 14 shows the CDF for the achieved throughput of P_1 and P_2 under the two strategy profiles. The throughput in the case of (HD, HD) is, on average, higher than that in the case of (FD, FD). Second, we repeat the same experiment under the *low self- and external interference* (LSEI) case, where we place two USRPs (c and d) outside the lab and the other two inside the lab. We also adjust the positions of the antennas to reduce the RSI signal. Under this scenario, as shown in Figure 15, the (FD, FD) strategy profile results in a much higher throughput compared to (HD, HD).

V. Conclusions

In this paper, we developed a novel Bayesian game-theoretic framework to study the coexistence problem between two FD-capable wireless links, where nodes have heterogeneous SIC capabilities. Although the throughput of a single link enhances significantly when operating in the FD mode, the additional caused interference (compared to the HD case) may limit its coexistence with a neighboring link. Our analysis revealed that the SIC capability of each link (which is the type of each player) has a double-threshold structure, i.e., the range of the SIC values can be divided into three regions. When the SIC capability is very good, operating in the FD mode strictly dominates the HD mode, whereas when the SIC capability is very poor, operating in the HD mode strictly dominates the FD mode. When the SIC capability is in the middle region, we derived the conditions on the probability distribution of the types of the other link under which HD (FD) strictly dominates FD (HD).

Our conducted experiments corroborated that FD is not always the optimal operation mode when considering an FD-enabled wireless network. The optimal mode of a link depends on (i) the external interference it encounters from neighboring links (which is a function of their transmission powers and channel gains) and (ii) its residual self-interference (which is a function of its SIC capability, its transmission power, and its channel gain). Given that the external interference will not be known a priori, a link relies on the probability distribution over the types of the other link in deriving its strategy. Our simulations demonstrated the impact of the residual self-interference and external interference on the received constellation diagram, and hence the BER. As future research, we plan to extend the proposed Bayesian game into more than two links, where each link does not know the exact SIC capabilities of the neighboring links. We will also investigate a power control scheme to be used as part of the game, in addition to FD/HD mode selection.

References

[1] A. Sabharwal, P. Schniter, D. Guo, D. W. Bliss, S. Rangarajan, and R. Wichman, "In-band full-duplex wireless: Challenges and opportunities," *IEEE Journal on Selected Areas in Communications*, vol. 32, no. 9, pp. 1637–1652, September 2014.

[2] D. Bharadia, E. McMilin, and S. Katti, "Full duplex radios," in *Proceedings of the ACM SIGCOMM Conference*, 2013, pp. 375–386.

[3] X. Xie and X. Zhang, "Does full-duplex double the capacity of wireless networks?" in *Proceedings of the IEEE INFOCOM Conference*, 2014, pp. 253–261.

[4] M. Duarte, A. Sabharwal, V. Aggarwal, R. Jana, K. Ramakrishnan, C. W. Rice, and N. Shankaranarayanan, "Design and characterization of a full-duplex multiantenna system for WiFi networks," *IEEE Transactions on Vehicular Technology*, vol. 63, no. 3, pp. 1160–1177, 2014.

[5] Y. Yang, B. Chen, K. Srinivasan, and N. B. Shroff, "Characterizing the achievable throughput in wireless networks with two active RF chains," in *Proceedings of the IEEE INFOCOM Conference*, 2014, pp. 262–270.

[6] C. Nam, C. Joo, N. B. Shroff, and S. Bahk, "Power allocation with inter-node interference in full-duplex wireless OFDM networks," Tech. Rep., 2014. [Online]. Available: http://netlab.snu.ac.kr/~cwnam/PowerControl.pdf

[7] D. N. Nguyen and M. Krunz, "Be responsible: A novel communications scheme for full-duplex MIMO radios," in *Proceedings of the IEEE INFOCOM Conference*, 2015, pp. 1733–1741.

[8] W. Afifi and M. Krunz, "Exploiting self-interference suppression for improved spectrum awareness/efficiency in cognitive radio systems," in *Proc. of the IEEE INFOCOM'13 Conf.*, Turin, Italy, Apr. 2013, pp. 1258–1266.

[9] ——, "Incorporating self-interference suppression for full-duplex operation in opportunistic spectrum access systems," *IEEE Transactions on Wireless Communications*, vol. 14, no. 4, pp. 2180–2191, April 2015.

[10] M. J. Abdel-Rahman, M. AbdelRaheem, A. B. MacKenzie, K. Cardoso, and M. Krunz, "On the orchestration of robust virtual LTE-U networks from hybrid half/full-duplex Wi-Fi APs," in *Proceedings of the IEEE WCNC Conference (to appear)*, 2016.

[11] M. J. Abdel-Rahman, M. AbdelRaheem, and A. B. MacKenzie, "Stochastic resource allocation in opportunistic LTE-A networks with heterogeneous self-interference cancellation capabilities," in *Proceedings of the IEEE DySPAN Conference*, 2015, pp. 200–208.

[12] W. Afifi, M. J. Abdel-Rahman, M. Krunz, and A. B. MacKenzie, "Coexistence in wireless networks with heterogeneous self-interference cancellation capabilities," University of Arizona, Department of ECE, TR-UA-ECE-2016-1, Tech. Rep., 2016. [Online]. Available: http://www2.engr.arizona.edu/~krunz/publications_by_type.htm#trs

[13] M. Duarte and A. Sabharwal, "Full-duplex wireless communications using off-the-shelf radios: Feasibility and first results," in *Proceedings of the IEEE ASILOMAR Conference*, 2010, pp. 1558–1562.